Thermally stimulated desorption of neutral CF3 from CF3I on Ag(111)

K. H. Junker, Z.-J. Sun, T. B. Scoggins, and J. M. White

Citation: The Journal of Chemical Physics **104**, 3788 (1996); doi: 10.1063/1.471032
View online: http://dx.doi.org/10.1063/1.471032
View Table of Contents: http://scitation.aip.org/content/aip/journal/jcp/104/10?ver=pdfcov
Published by the AIP Publishing

Thermally stimulated desorption of neutral CF_3 from CF_3I on Ag(111)

K. H. Junker, Z.-J. Sun,[a] T. B. Scoggins, and J. M. White
Department of Chemistry and Biochemistry, University of Texas at Austin, Austin, Texas 78712

(Received 26 September 1995; accepted 28 November 1995)

The low temperature thermal chemistry of CF_3I on Ag (111) presents an example of competing reaction pathways; molecular desorption vs desorption of radical CF_3. Temperature programmed desorption and angle resolved temperature programmed desorption, complemented with Auger electron spectroscopy and low energy electron diffraction, were used to discern the mechanism of the CF_3 radical desorption channel. CF_3 desorption is limited to the first monolayer of CF_3I; 0.75 ML CF_3I is the coverage used for angular dependence measurements. At 90 K most of the CF_3I adsorbs molecularly to the metal, but also present under these conditions are dissociative adsorption and thermal decomposition channels limited to C–I bond cleavage. The decomposition product, CF_3, desorbs as a radical at high temperatures (~320 K) with the I remaining on the surface until 850 K. At submonolayer CF_3I coverages, thermal activation produces a low temperature (100–150 K) radical desorption channel. Results indicate that low temperature CF_3 thermal desorption occurs via dissociative electron attachment to molecular CF_3I, yielding radical CF_3 and adsorbed iodine. © *1996 American Institute of Physics.* [S0021-9606(96)03109-0]

I. INTRODUCTION

Current technological and environmental interests have motivated recent studies of simple halocarbons on surfaces. Fluorocarbons are used as lubricants and chemical etchants and are significant atmospheric pollutants. One of the simplest of these, CF_3I, is used in fire extinguishing materials, but has also attracted much attention as a possible threat to the ozone layer.[1] In addition, gas phase electron attachment studies[2–5] have shown the promise of CF_3I in varied applications from threshold ion detection to trace detection of drugs and explosives.[3] Currently, there is additional interest in the chemical comparison of CH_nX and CF_nX (X=Cl, Br, and I) molecules on surfaces because of their substantial difference in electron affinities and reversed dipoles, i.e., the dipole moments lie in the direction of the X and CF_n groups, respectively.

Previous studies have reported the thermal desorption of CF_3I from metal surfaces,[6–10] including clean and iodine-precovered Ag(111).[11] Like the other coinage metals, Ag has a filled *d*-electron valence band which makes it a comparatively nonreactive transition metal. With the CF_3I/Ni(100) system, Thiel and co-workers have observed complete dissociation of CF_3I in TPD, including formation and desorption of NiF_2.[8] Myli and Grassian observe NiF_2 formation under thermal activation of CF_3I on both Ni(100) and Ni(111).[10] Other studies have observed both C–I and multiple C–F bond scission on Pt(111) and Ru(001).[7,9] In contrast, with CF_3I on Ag(111), dissociation has been shown to be limited to C–I bond breaking. Neither is there any evidence for C–C bond formation.

Focusing on the low temperature regime (<150 K), we have re-examined the thermal desorption of CF_3I on clean and I-precovered Ag(111). In addition to low temperature molecular desorption, we find new experimental evidence for a low temperature CF_3 radical desorption channel. Temperature programmed desorption (TPD) and angle resolved temperature programmed desorption (ARTPD), coupled with Auger electron spectroscopy (AES) and low energy electron diffraction (LEED), were used to discern the mechanism of the CF_3 radical desorption channel. Bent and co-workers have recently observed a similar CH_3 radical desorption from CH_3I adsorbed on Cu(111);[12] their proposed mechanism involves atom transfer to and/or electron transfer from the surface to the adsorbed CH_3I. We believe both molecular orientation in the first layer and electron attachment from the surface play large roles in the CF_3 desorption mechanism.

Substrate electron transfer is a vital pathway to molecular photodesorption/photodecomposition of adsorbates on surfaces.[13,14] Such transfer to CF_3I from Ag(111) is important in photon induced desorption (193 and 248 nm) of CF_3 radicals.[15] Typically, the photon is adsorbed by the substrate, creating an excited electron that remains below the vacuum level. The hot electron can then attach itself to an unoccupied state of the adsorbed molecule, given the appropriate energetics and spatial location and orientation. Depending upon the work function of the system and the electron affinity of the adsorbed molecule, the energy required to attach an electron from the substrate to the adsorbate can approach thermal energies.

In the work reported here, a model for *thermally*-activated electron transfer, similar to harpooning in classical gas phase crossed beam experiments,[16] is presented to explain the low temperature radical desorption of CF_3 from Ag(111). Incorporating results of gas phase dissociative electron attachment (DEA) studies of CF_3I, our evidence supports the mechanism of electron transfer from the surface to CF_3I, dissociatively ejecting neutral CF_3.

[a]Present address: Department of Chemistry, University of Pennsylvania, 231 S. 34th St., Philadelphia, Pennsylvania 19104.

 0021-9606/96/104(10)/3788/9/$10.00

II. EXPERIMENT

The experiments were performed in two separate ultrahigh vacuum chambers. The initial work was done in a chamber described in detail elsewhere.[17] Briefly, this system is equipped with a quadrupole mass spectrometer (EXTREL), an ion gun for sputtering, and AES to check surface cleanliness. The mass spectrometer was differentially pumped and separated from the main chamber by an aperture with an i.d. of 3 mm. The sample was liquid nitrogen cooled to a temperature of 90 K and could be resistively heated to the melting point of silver, greatly reducing background adsorption on the sample leads. This dosing technique produces identical CF_3I TPD results to microcapillary dosing[11] and backfilling techniques.[21] CF_3I was dosed through a 10 μm pinhole doser terminating within 1 mm of the surface. The sample was cleaned by Ar^+ ion sputtering and subsequent annealing at 690 K. The base pressure in the chamber is 3×10^{-10} Torr.

The ARTPD spectra were acquired in a separate two-level UHV chamber.[18] The main feature of this system is a 360°-rotatable differentially pumped quadrupole mass spectrometer (EXTREL). This chamber is equipped with both AES and a reverse-view LEED to check surface composition and order, respectively. The sample temperature was controllable between 85 K and the melting point of silver; the base pressure of the system was 8×10^{-11} Torr. The Ag(111) crystal was cleaned in the manner described above until no impurities were seen by AES and a sixfold LEED pattern was obtained. The sample was cleaned after every TPD to remove remaining iodine from the surface.

CF_3I coverages are based upon previously published work;[11,15] monolayer coverage is defined as the saturation of all peaks prior to the onset of the multilayer peak at 101 K in the I^+ TPD spectrum. Assuming a constant sticking coefficient, TPD of 1 ML produces a 1:1 ratio of parent to dissociated CF_3I, i.e., 0.50 ML desorption of molecular CF_3I. This value differs from a previous estimate, which did not account for low temperature CF_3 desorption.[15] This point will be discussed further in Sec. III.

Cracking ratios for CF_3 radicals in the QMS, determined from the known 320 K CF_3 desorption peak in the TPD spectrum, are $CF_3^+:CF_2^+:CF^+=1:5.6:5.6$. Molecular CF_3I cracking ratios were found by desorbing CF_3I from a surface saturated with iodine, insuring only molecular adsorption and desorption of CF_3I.[11] The relative CF_3I fragmentation ratios with our mass spectrometer were found to be $CF_3I^+:I^+:CF_3^+:CF_2^+:CF^+:F^+=100:120:83:29:11:9$, compared to 100:96:77:7:12:15 in the literature.[19] Monolayer I on Ag(111) was verified by a saturated atomic I_{511}/Ag_{356} Auger ratio of 0.11 (0.33 I/Ag atomic ratio) and a $\sqrt{3}\times\sqrt{3}R30°$ LEED pattern.[20]

III. RESULTS

A. Temperature programmed desorption

1. Molecular CF_3I desorption

Figure 1, previously published elsewhere,[15] shows the CF_2^+ ion signal in the TPD spectrum of multilayer CF_3I dosed on clean Ag(111). The heating rate was 4 K/s; the dosing temperature was 90 K. Visible are peaks attributed to monolayer molecular desorption at 120 K (α_2) and 128 K (α_3). At low coverages, the α_4 peak is resolved as a broad feature at 140 K. Upon adding CF_3I, a new peak at 128 K (α_3) appears. Both the α_3 and α_2 peaks are saturable. These results are in agreement with the work of Castro *et al.*,[11] however, it should be noted that multilayer formation occurs below their reported base sample temperature. Multilayer desorption (α_1) begins at 101 K, but shifts to 105 K and is nonsaturable. CF_3I^+ and CF^+ signals also peak at these temperatures. Two decomposition channels, both involving C–I bond scission are observed; these are outlined in the following sections. As in earlier results, no evidence of C–F bond cleavage or C–C bond formation was seen.

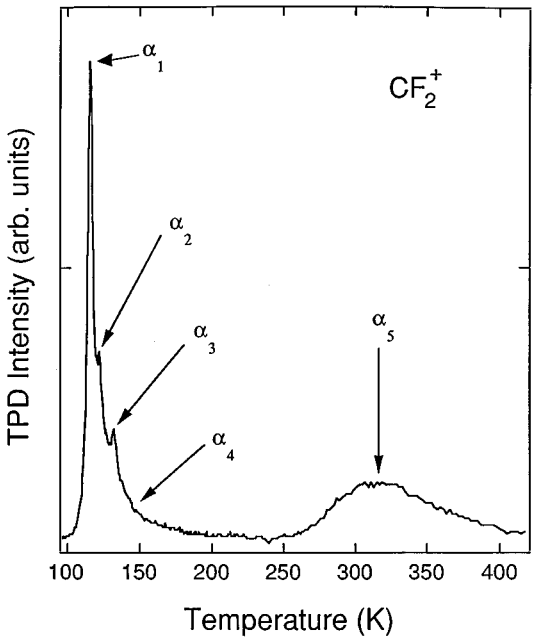

FIG. 1. TPD spectrum of the CF_2^+ ion for 3 ML CF_3I on clean Ag(111). Saturation of the α_2 peak is defined as the monolayer. The α_1 peak is not saturable under the present experimental conditions. No I^+ desorption coincides with the α_5 peak, therefore, this peak is assigned to a thermal decomposition product, CF_3. I^+ desorbs between 750–900 K. Taken from Ref. 15.

On the I-passivated surface, monolayer CF_3I grows in at 126 K; the multilayer initially comes in at 102 K but shifts to 108 K with increasing coverage and is nonsaturable up to 10 ML. For all coverages, the fragmentation pattern is that for molecular CF_3I, i.e., in agreement with previously published results,[11,15] there is no molecular decomposition.

2. High temperature CF_3 desorption

A major feature in Fig. 1 is a CF_3 desorption peak centered at 320 K (α_5), where no I^+ or CF_3I^+ was seen. As the coverage increases, this peak broadens and shifts to lower temperatures but saturates at a coverage of 1 ML CF_3I. As discussed previously, these uptake characteristics suggest a repulsive interaction between neighboring CF_3 groups on the

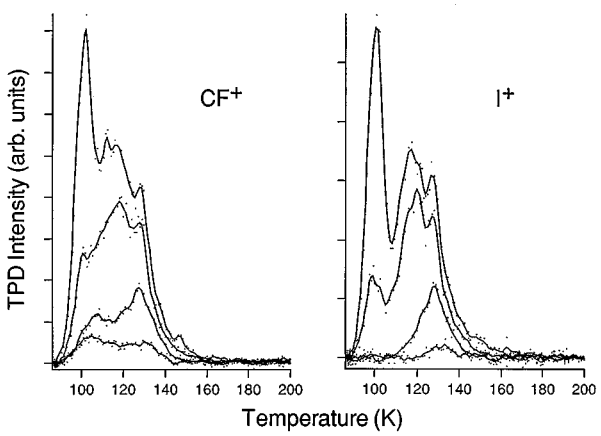

FIG. 2. Low temperature, 100–200 K, TPD spectra of CF^+ and I^+ ions for increasing coverages (bottom to top). The onset of the multilayer peak at ~100 K prior to saturation of the monolayer states is indicative of molecular island formation on the surface. The CF^+ peak at 110 K, not present in the I^+ fragment spectra, is due to low temperature CF_3 radical desorption.

surface.[11] We believe that the larger portion of these radicals is formed by decomposition of the parent as the substrate is heated. Atomic iodine desorbs at 850 K (not pictured).

3. Low temperature CF_3 desorption

Figure 2 shows two new features observed for thermal desorption of low coverage CF_3I on Ag(111). The ramp rate was slowed to 3 K/s to separate the different low temperature desorption channels. The first important feature in the spectra is the growth of multilayer CF_3I before the saturation of the monolayer, and/or bilayer indicating probable growth of three-dimensional CF_3I clusters on the surface. Secondly, the slower heating rate unveiled, particularly at low coverages, a CF^+ fragment peak at ~110 K that is absent in the I^+ fragment of CF_3I but does appear in the CF_2^+ spectra (not pictured). This is emphasized in Fig. 3 (top) for 0.96 ML CF_3I. The peak attributed to CF_3 radical desorption is labeled in the CF^+ spectrum, but is not present in the I^+ signal.

While the presence of an additional peak in the CF^+ spectra suggests desorption of CF_x species, two possibilities could account for the abrupt increase of the CF^+ signal; (1) formation of a CF_2 radical, as seen with CF_3I on Pt(111),[7] or (2) the cracking of the CF_3 radical into CF_2. Since there is no evidence for decomposition on Ag(111) beyond C–I bond scission, the observed abrupt increase in CF_2^+ signal must arise from the cracking of CF_3 radicals. Further evidence is obtained by comparing the CF^+ and CF_2^+ intensities after subtraction of the parent molecule cracking contribution. The CF^+ signal exactly overlaps the CF_2^+ signal once the parent molecule cracking portion is subtracted and the resulting areas are corrected for the cracking ratio of CF_3.

As defined in Sec. II, TPD of 1 ML CF_3I results in an estimated 0.5 ML of molecular CF_3I desorption and 0.5 ML of CF_3I, which dissociates upon heating. Based on a direct comparison of CF^+ fragment intensities for the low and high temperature CF_3 radical desorption channels, their coverages are estimated at 0.27 ML and 0.23 ML, respectively. Thus,

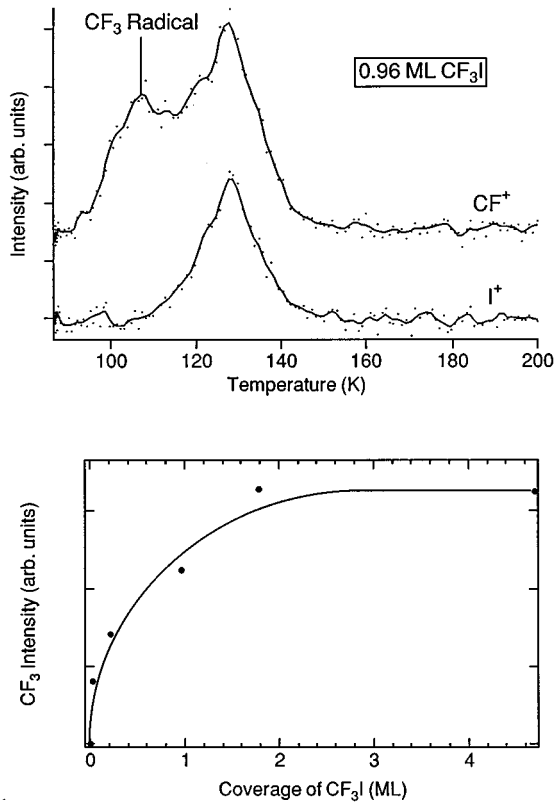

FIG. 3. (Top) CF^+ and I^+ ion signals for 0.96 ML CF_3I on Ag(111). The peak designated as CF_3 radical desorption appears at ~110 K in CF^+ spectrum, but is absent in the I^+ fragment signal. (Bottom) Desorption yield of CF_3 as a function of total coverage. CF_3 yields are determined by subtracting the molecular contribution from the CF^+ fragment intensity. A coverage of ~1.5 ML CF_3I completely saturates both the first monolayer of CF_3I (desorption up to the onset of the multilayer peak) and the low temperature CF_3 radical desorption channel.

saturated low temperature CF_3 radical desorption corresponds to 0.27 ML parent desorption. Sun *et al.* recently reported that an initial coverage of 1 ML CF_3I on Ag(111) generated 0.70 ML molecular CF_3I desorption in TPD.[15] The remaining 0.30 ML was attributed to the high temperature CF_3 radical channel. In their results, however, the low temperature CF_3 desorption channel was not separated from molecular CF_3I. Using our data, combining molecular desorption and low temperature CF_3 desorption gives 0.77 ML, in reasonable agreement with previous work.

Figure 3 (bottom) is a plot of the low temperature CF_3 desorption intensity (CF^+) as a function of dosed CF_3I coverage. The radical desorption is present at low coverages (<0.1 ML), and quickly rises until the coverage reaches approximately 1.5 ML, where it saturates. Note that due to the presence of CF_3I clusters, the multilayer contributes to the overall intensity before the first layer is complete. Therefore, a saturated monolayer, as defined in Sec. II, is not achieved until the total coverage is ~1.5 ML. The TPD CF_3 radical desorption signal fits a first order dissociative process with the pre-exponential factor lying between 10^{11} to 10^{15} s^{-1} and an activation energy of 6.5 kcal/mol (0.28±0.05 eV).

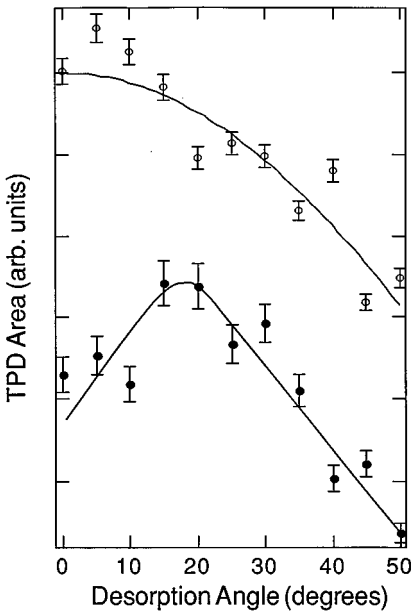

FIG. 4. ARTPD distribution curves for CF_3 (lower curve) and CF_3I (upper curve) for 0.75 ML CF_3I on Ag(111). The solid points are the averaged CF^+ and CF_2^+ intensities at low temperatures (100–150 K) minus the molecular contribution. The smooth curve is a guide to the eye. The I^+ fragment (open circles) originates strictly from molecular CF_3I at <150 K. The upper smooth curve is a cosine plot.

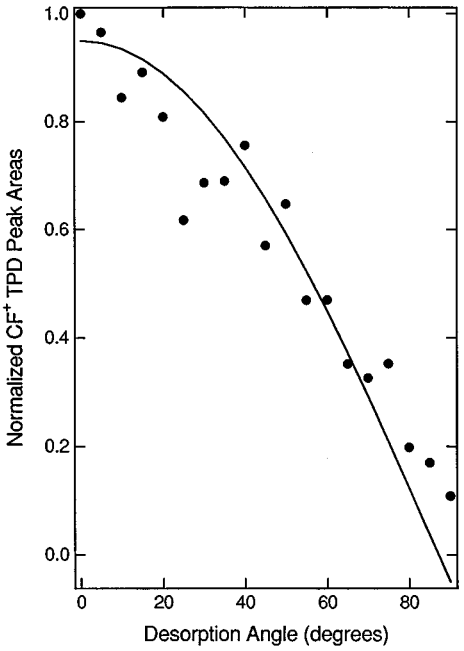

FIG. 5. ARTPD distribution curve for the 320 K CF_3 desorption feature. Areas are normalized to the CF_3 desorption normal to the surface (0°). The line is a cosine plot through the data.

4. Radical desorption from I-passivated surface

In contrast, neither CF_3 desorption channel was observed on an I-precovered Ag(111) surface. The desorption of CF_3I from I-passivated Ag(111) was carefully monitored, specifically at less than 1 ML coverage. The molecular cracking ratio is initially determined from the cracking signals at a high coverage of CF_3I (>3 ML) and is reported in Sec. III A 1. At this coverage, contributions from CF_3 to the relative intensities of the fragments will be negligible since the chemistry that leads to this desorption channel apparently occurs in the first monolayer. Regardless, the CF^+ and I^+ thermal desorption profiles tracked each other; in addition, their cracking ratio CF^+/I^+ did not change with coverage, indicating desorption of only molecular CF_3I.

B. Angle-resolved temperature programmed desorption

ARTPD results for 0.75 ML CF_3I are pictured in Fig. 4; at this coverage, the 110 K CF_3 radical signal is most easily separated from the parent desorption. Angle-dependent TPD measurements were collected from 0.5–0.85 ML CF_3I; all displayed the same angular features. Plotted are the TPD areas, between 90 and 150 K, for both molecular CF_3I and neutral CF_3 desorption fragments versus desorption angle (relative to the surface normal). All areas are normalized to the I^+ fragment area at $\theta=0°$. The upper points (open dots) follow the I^+ fragment of molecular CF_3I desorption between 100–150 K. The smooth curve is a $\cos(\theta)$ plot through the points. The lower points (filled dots) are an average of the CF^+ and CF_2^+ signals from ejected CF_3 corrected for fragmentation and for CF_3I contributions. The smooth curve serves to guide the eye. The desorption maximum for CF_3 falls between 15°–20° off normal and is not present for molecular CF_3I desorption, providing further evidence that radical CF_3 is desorbing in this low temperature regime.

ARTPD was also performed on the high temperature (320 K) radical CF_3 desorption channel (Fig. 5). In contrast to its behavior at lower temperatures, the CF_3 desorption peaked normal to the surface ($\theta=0°$) with a $\cos(\theta)$ drop in intensity with increasing angle.

Finally, despite the lack of observable CF_3 desorption, ARTPD spectra were taken for 0.75 ML CF_3I coverage on I-passivated Ag(111). Consistent with the earlier uptake curves taken at the surface normal, the CF^+ and I^+ fragment intensities tracked one another and their ratio (CF^+/I^+) did not change with desorption angle, again indicating the absence of radical CF_3 formation on this surface.

IV. DISCUSSION

Our TPD and AES results agree with the previously published thermal chemistry of CF_3I on Ag(111) (Ref. 11) except for the observation of the low temperature CF_3 radical desorption. At 90 K, the majority of CF_3I molecules adsorb intact on Ag(111); true multilayer formation is observed which was not attainable at adsorption temperatures greater than 100 K.[11] Fourier transform infrared (FTIR) spectroscopy results indicate that at this sample temperature a portion of the CF_3I molecules, estimated at 10% of a monolayer, dissociate upon adsorption.[21] Upon heating the crystal, two distinct dissociation pathways appear; dissociation with the

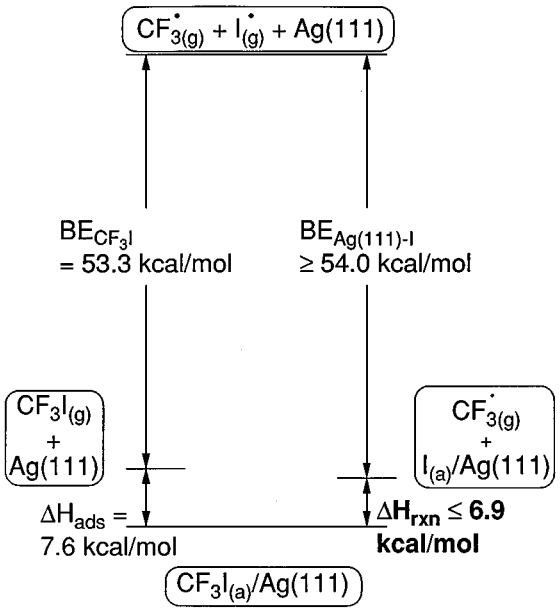

FIG. 6. A thermochemical cycle for the desorption of CF_3 radicals from CF_3I/Ag(111). The enthalpy of formation of $CF_{3(g)}$ is estimated to be ≤6.9 kcal/mol.

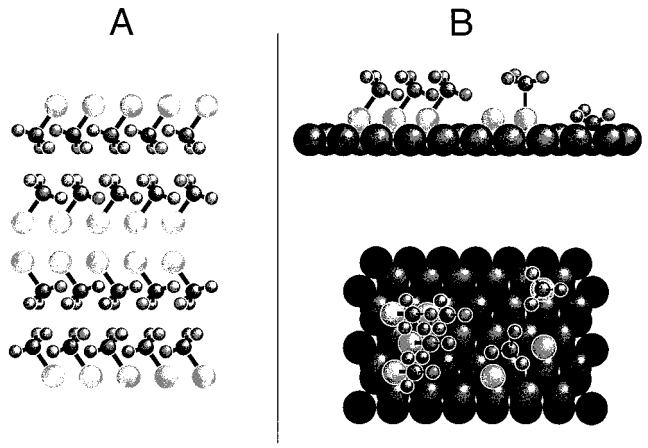

FIG. 7. (a) The solid state crystalline form of CF_3I in the temperature range 115–140 K. Alternating molecules within each row and column lie slightly in and out of the plane of the figure. (b) Side and top views for the proposed bonding structure for first layer CF_3I on Ag(111). All bonding is pictured on threefold hollow sites. In this temperature and coverage range, CF_3I lone molecules and clusters, CF_3 molecules, and I atoms all exist on the surface.

fragments retained on the surface and CF_3 radical ejection into the gas phase. According to a previous model,[11] some of the CF_3I molecules that adsorb in the Ag threefold hollow sites, *without* an atom underneath, dissociate upon adsorption into $CF_{3(ad)}$ and $I_{(ad)}$. Some or all of the remaining molecules in these sites dissociate upon heating the crystal. This adsorption pathway is site limited, i.e., it saturates at 1 ML coverage of CF_3I. The molecules that adsorb in the threefold sites *with* an Ag atom beneath do not dissociate. This model is consistent with our coverage assignments (1:1 ratio of molecular to radical desorption assuming equal occupancy) as well as with what we see for I-precovered Ag. This model, however, does not discriminate between the low and high temperature CF_3 radical desorption channels we observe in the current study, and it is the low temperature channel to which we now turn.

Based on a simple thermodynamics calculation, we can estimate the energy required for CF_3 desorption directly to the gas phase. Consider the reaction

$$CF_3I_{(g)} \rightarrow CF_3I_{(ad)},$$
$$CF_3I_{(ad)} + Ag_{(s)} \rightarrow CF_{3(g)} + Ag\text{–}I_{(ad)}. \quad (1)$$

The thermodynamic threshold for this reaction is estimated from a Born–Haber cycle (Fig. 6). The gas phase C–I bond dissociation energy of CF_3I is well established at 53.3 kcal/mol (2.31 eV). The Ag–I bond energy, estimated from Redhead analysis[22] of the thermal desorption of atomic I from Ag(111) at 850 K, is 54.0 kcal/mol (2.35 eV).[11,15] Added to the cycle is the heat of adsorption of CF_3I. The upper limit of 7.6 kcal/mol (0.33 eV) for this value is calculated from the molecular desorption peak at 128 K, assuming a preexponential factor of 10^{13} s^{-1}. Therefore, the enthalpy change for the formation of CF_3 radicals is $\Delta H_{rxn} \leqslant 6.9$ kcal/mol (0.30 eV). Interestingly, this value is within the uncertainty of the activation energy for low temperature CF_3 desorption.

The observation of CF_3 radicals ejected ~18° off the surface normal at 110 K, however, is not consistent with a purely thermally driven desorption mechanism. Referring to Fig. 5, CF_3 radicals that desorb from the *substrate* leave as the cosine of the intensity normal to the surface. Molecular CF_3I desorption also follows the cosine drop-off in intensity with desorption angle (Fig. 4), making it unlikely that the off-normal desorption maximum in the ARTPD of low temperature CF_3 originates from an adsorbed state on the surface. We suggest instead that low temperature CF_3 desorption originates from a nonthermal process that cleaves the C–I bond, ejecting CF_3 into the gas phase.

A. CF_3I structure on Ag(111)

The angular dependence plot of the CF_3 desorption implies that CF_3I is in a tilted position at the instant the CF_3 radical is released. Castro *et al.* suggest that the first monolayer of CF_3I adsorbs molecularly with the iodine down in accord with the adsorption behavior of CH_3I.[11] FTIR spectra indicate that CF_3I molecules initially adsorb parallel to the surface, but stand upright as the coverage is increased up to a monolayer.[21] Recent neutron powder diffraction studies have singled out two distinct solid phases of CF_3I with the phase transition at 115 K.[23] The melting point of the higher temperature phase I, depicted in Fig. 7(a), is 143 K. Phase II is presumed to be a lower symmetry, distorted form of the phase I structure. Phase I is dominated in the crystal structure by soft I–I and hard F–F interactions. Similar interactions for CF_3I gas phase clusters have been calculated elsewhere.[24] The predominant molecular libration is a coincident C–I bond stretch and 21° rotation of the CF_3 group about the C–I axis. The displacement of the C–I bond from its solid state

equilibrium distance during this jump rotation is estimated to be ~1.5%. The tilt of the molecule with respect to the plane containing iodine atoms is 34.5° off normal. The distances between iodine atoms in the crystal are 3.95 and 4.61 Å.

The distance between equivalent threefold sites available for molecular adsorption on Ag(111) is 4.98 Å.[25] If CF_3I formed a two dimensional structure on the surface similar to crystalline CF_3I, we would not expect an identical packing density, but the interactions between adjacent molecules could easily be strong enough to force the C–I axes to tilt on the surface. Indeed, at coverages where CF_3 radical desorption is observed, FTIR results indicate that a significant fraction of the CF_3I molecules are tilted on the surface.[21] Figure 7(b) represents the proposed bonding geometries of first layer CF_3I molecules on Ag(111) in the temperature range 90–150 K. At these temperatures, both dissociated and isolated CF_3I molecules along with groups of CF_3I islands are thought to be present on the surface. Lone CF_3I molecules may adsorb with their molecular axes anywhere from parallel to perpendicular to the surface plane. As the molecules cluster, the interactive forces between neighboring molecules cause the molecular axes to tilt. Iodine atoms are pictured on the threefold sites without an Ag atom underneath, their bonding sites on an iodine saturated surface.[25] Molecular CF_3I can exist on both sites, either with or without a next layer atom, but the island in Fig. 7(b) is located on those without atoms directly beneath. The adsorbed CF_3 group is also pictured on the threefold site without an underlying Ag atom; however, there is no evidence for or against this adsorption site. Note at this point that the onset of CF_3 desorption is within 5 K of the reported phase transition. We believe the molecular orientation, and possibly the phase transition, of adsorbed CF_3I are important in the radical ejection mechanism.

B. CF_3 radical formation

Assuming for now that the molecule resides in a tilted configuration on the surface, we next focus on the driving force to cleave the C–I bond. Having already shown that the formation of the radical requires at most 0.28 eV, consider the mechanism to overcome this activation barrier. There are at least three possibilities; first, either the substrate interaction with the adsorbate's potential energy surfaces or neighboring interactions between molecules could orient the CF_3I molecules, so that the radicals eject off-normal during dissociation. The radicals would have to desorb on a short enough time scale and with enough translational energy to retain, in their angular distribution, the characteristics of the oriented CF_3I molecule, i.e., the tilt. Alternatively, the C–I coordinate potential may depend strongly on the C–I axis angle with respect to the surface normal. In this case, the energetically lowest pathway to dissociation would reside at the appropriate angle, i.e., 15°–20° off-normal. Once the activated complex position is reached, depending on the shape of the potential surface and the time scale for cleaving the C–I bond, dissociation in these scenarios would lead to the observed product angular distribution. However, it is difficult to imagine, based on the solid state structure of CF_3I, that a 20° tilt alone would activate the C–I bond.

A final, and we believe more likely, explanation for the radical desorption is dissociative electron attachment (DEA) from the surface to the CF_3I molecule, causing ejection of CF_3 into the gas phase. The lifetime of an EA event on the surface is at least several orders of magnitude shorter than vibrational motion leading to thermal desorption,[26] thus allowing CF_3 ejection to take place along the initial C–I bond direction.

As alluded to earlier, the gas phase DEA of CF_3I has been well studied in the literature.[2–5] There are two significant resonances below 5 eV. The weaker of the two, at 4 eV, generates a combination of CF_3^-, F^-, and FI^- and their complementary neutral fragments I, CF_2I, and CF_2, respectively.[4] None of these were observed in our experiment. By far the stronger resonance is through the σ^*(C–I) antibonding orbital

$$e^- + CF_3I \rightarrow CF_3 + I^- \tag{2}$$

at or near 0 eV; it produces copious amounts of I^-. The cross section for this reaction at thermal energies (<30 meV) is *at least* 10^{-14}–10^{-13} cm^2.[3,4] The calculated thermodynamic threshold for reaction (2) is −0.75 eV (~17 kcal/mol), the excess energy being carried away in product translational modes.[4,5] Adding the energy gained from reaction (2) to reaction (1), and assuming entropy is changing in our favor, then forming CF_3 radicals becomes thermodynamically favored provided electron attachment is energetically possible, i.e., the attachment resonance is sufficiently below the vacuum level to make the EA probability measurable.

A schematic of the potential energy curves for CF_3I and its anion adsorbed on Ag(111) are shown in Fig. 8. Because gas phase CF_3I captures thermal electrons, the anion potential energy surface (PES) crosses through the neutral PES near its ground vibrational state. The PES well depth of the anion (in the gas phase) is defined as the electron affinity of CF_3I (1.57 eV).[4] As stated previously, the estimated lower limit for the adsorption enthalpy of CF_3I is 7.6 kcal/mol (0.33 eV). To properly define the total energy of the CF_3I/Ag(111) system, all energies are referenced to the Fermi level, the state with CF_3I adsorbed on the Ag(111) substrate. The work function is the energy required to remove an electron from this state to infinity. Although the work function change of Ag(111) upon adsorption of CF_3I is not known, ~1 ML coverage of CF_3I on Pt(111) lowers its work function at 100 K by 0.6–0.7 eV.[7] The work function of clean Ag(111) is 4.74 eV,[27] based on the CF_3I/Pt(111) system, we will assume the work function of the Ag metal is lowered to 4.1 eV at the coverage of interest.

Following previously derived equations describing substrate electron transfer,[12,13] an estimation of the electron energy needed for DEA is

$$E_D = \Phi - \mathrm{VEA}[CF_3I_{(ad)}], \tag{3}$$

where Φ is the work function of the CF_3I/Ag(111) complex and VEA is the vertical electron affinity, in this case, of the

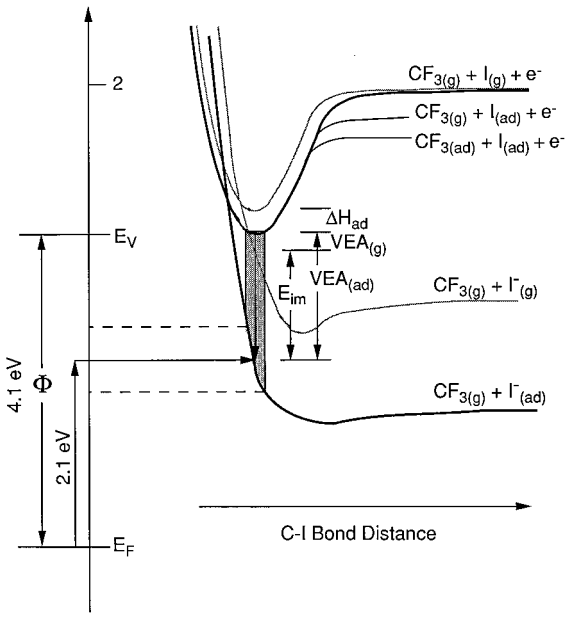

FIG. 8. A schematic of the potential energy curves for the CF_3I/Ag(111) system. The bold curves represent the ground state neutral and anion curves for adsorbed CF_3I. The lighter penned curves are the corresponding surfaces for the gas phase molecule. The Fermi energy, E_F, is located for the state where CF_3I is adsorbed on the surface; the work function is the energy required to remove an electron from this state. The anion potential crosses the ground state surface in a region at or near the ground vibrational energy, indicating gas phase attachment of near zero kinetic energy electrons. 2.1 eV is the most probable energy required for attachment to the broadened ground state wave function projected along the anion curve.

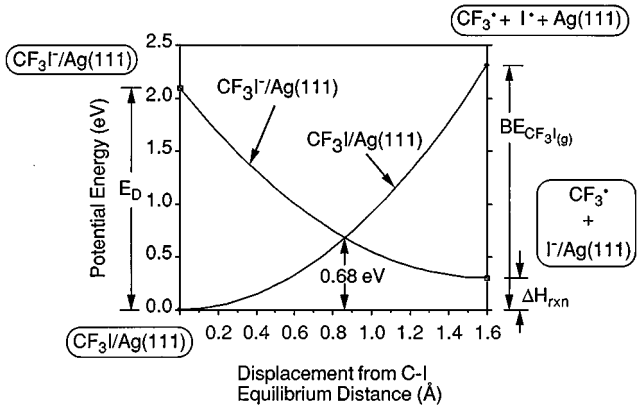

FIG. 9. Plot of potential energy for CF_3I/Ag and CF_3I^-/Ag as a function of C–I bond separation. The left axis is the energy calculated for electron attachment, 2.1 eV. The right axis has an upper bound given by the gas phase dissociation energy of CF_3I and a lower limit of the ΔH_{rxn}, 0.30 eV. A typical van der Waals separation of 1.6 Å is used as the maximum displacement of the atoms from equilibrium. The point at which the curves cross (0.68 eV) is the minimum energy required for electron attachment to the adsorbate.

adsorbed molecule. The vertical electron affinity is defined as the energy difference between a molecule in its ground electronic, vibrational and rotational states plus an electron at infinity and the negative ion formed by attachment while holding the internuclear configuration fixed.[28] By strict definition, the VEA of CF_3I might be more accurately referred to as the vertical detachment energy (VDE) (Ref. 28) because the EA value for this molecule is estimated to be 0.0–0.5 eV *positive* in the gas phase.[29] Referring to Fig. 8, a positive VEA energy implies that the anion curve lies beneath the ground state surface in the Franck–Condon region (shaded) for vertical attachment. For the purposes of this discussion, the terms VEA and VDE will be used interchangeably. By constructing a thermochemical cycle to model the attachment process, $\mathrm{VEA}[CF_3I_{(ad)}]$ can be written as

$$\mathrm{VEA}[CF_3I_{(ad)}] = \mathrm{VEA}[CF_3I_{(g)}] + E_{\mathrm{im}} + E_{\mathrm{pol}} + \delta. \tag{4}$$

The image charge stabilization, E_{im}, coupled with the stabilization due to the neighboring adsorbates, E_{pol}, lower the energy of the system. δ represents the correlation and exchange energy of the ion and the surface and is assumed to be negligible at distances corresponding to the weakly bonded, physisorption limit. Combining Eqs. (3) and (4) gives a formula using calculated or known experimental quantities for estimating the required substrate electron energy needed for DEA,

$$E_D = \Phi - \mathrm{VEA}[CF_3I_{(g)}] - E_{\mathrm{im}} - E_{\mathrm{pol}}. \tag{5}$$

E_{im} is given by $e^2/4z = (3.6/z)$ eV,[13] where z is the distance in angstroms of the charge from the surface plane. For $z = 2.5$ Å, a reasonable estimate for weakly adsorbed molecules, the value of E_{im} is 1.44 eV. E_{pol} can be estimated by using the electronic polarization energy of the anion in its liquid form.[13] For CF_3I coverages less than or equal to a monolayer on Ag(111), E_{pol} is estimated at 0.5 eV.[30] Using a minimum absolute value for $\mathrm{VEA}_{(g)}$ (0 eV), the VEA of adsorbed CF_3I is calculated to be approximately 2 eV. Therefore, the most probable electron energy for the DEA event is 2.1 eV.

As noted in the results section, a pre-exponential factor of $\sim 10^{13}$ s^{-1} gives a much lower activation energy, 0.28 eV, for CF_3 ejection. At this point, it is worthwhile to examine briefly how the activation energy varies as a function of C–I bond distance. Qualitatively, Fig. 8 shows that as this coordinate increases, the vertical attachment takes place on the anion curve at lower energies (<2.1 eV). This is shown more accurately in Fig. 9. After Lin and Bent,[12] we have plotted the energies of CF_3I/Ag(111) and CF_3I^-/Ag(111) vs the C–I bond coordinate. The anion repulsive curve is defined at the C–I equilibrium distance by the electron attachment energy, 2.1 eV, and at the dissociation limit by the heat of reaction, 0.30 eV. The gas phase bond dissociation energy defines the neutral harmonic curve at the C–I bond limit. The crossing point at 0.68 eV represents the minimum energy required for attachment of an electron from the metal. The energy E_D should also be considered an upper limit because a conservative estimate of 0.0 eV for the gas phase VEA value was used in its determination. Better estimates would, in all cases, lower the dissociative attachment energy.

Taking the above estimate still leaves ~0.7 eV activation energy required to promote and attach an electron to the adsorbate. Although this value is comparable to the activation energy estimated from TPD, the tilt of the molecule may

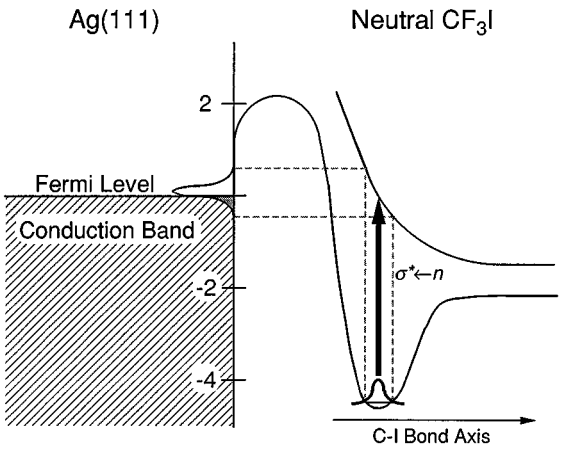

FIG. 10. Potential energy curves for the ground and first excited state of neutral CF_3I on Ag(111). The nonbonding state energy is defined relative to the Fermi level of Ag(111) based on UPS studies. The σ^* energy is based on gas phase UV absorption studies of CF_3I. The transition energy that lies within the Franck–Condon region, overlaps the Fermi energy of the metal, suggesting that electron attachment via tunneling to the adsorbate is energetically conceivable.

also play an important role. One effect of tilting the molecule on the surface is to alter the overlap of the iodine atomic orbitals with the metallic orbitals at the surface. Increasing the overlap could move the neutral curve of Fig. 8 towards the Fermi level. EA is strongly resonant, so consider the energy of the orbital to which the electron attaches in the neutral CF_3I molecule. From gas phase UV absorption studies,[31] the lowest unoccupied molecular orbital (LUMO) of CF_3I, the a_1 σ^*(C–I) antibonding orbital, lies slightly below that of CH_3I. For CX_3I molecules, the *A* absorption band arises from a $\sigma^*\leftarrow n$ $(5p\pi)$ transition. The onset of the $\tilde{A}\leftarrow\tilde{X}$ transition for CF_3I is at 4.41 eV,[31] i.e., the σ^*(C–I) orbital lies 4.41 eV above the iodine lone pair $4e$ orbitals. UPS studies of CF_3I adsorbed on clean Ag(111) (Ref. 11) show that the center of the $4e$ orbital energy lies approximately 4.6 eV below the Fermi energy of silver. Assuming a similar lowering and broadening of the LUMO, the σ^* onset would begin ~1 eV above the Fermi level of Ag(111) (Fig. 10). As the electron approaches the molecule during the attachment process, the electronic structure of the molecule becomes more like that of the anion. From final state arguments, the CF_3I^- MO is most likely slightly higher in energy than the corresponding neutral LUMO. Regardless, the optical transition places the LUMO near the Fermi level during EA. Since the energy levels of the adsorbate and the substrate are comparable, electron attachment via tunneling through the activation barrier is a possibility.

We suggest that as the molecules orient, and possibly undergo a phase change, they reach a ''critical orbital overlap'' with the Ag(111) metallic orbitals; at this angle an electron tunneling channel opens. The probability for electron tunneling through the potential barrier at the adsorbate/substrate interface increases as the adsorbate moves closer to the surface, hence the Ag–I coordinate becomes an important factor. Because decomposition of the parent leaves strongly bound iodine atoms on the surface, it is reasonable to assume at least the I atom moves to a more chemisorbed bonding configuration coincident with CF_3 low temperature desorption. At the very least the barrier for DEA would be lowered further. Regardless, it is from this ''tilted'' orientation that CF_3 radical desorption is observed at low temperatures; therefore, the orientation of the molecule seems to play a key role.

C. CF_3I on I-precovered Ag(111)

The absence of CF_3 radical formation at both low and room temperatures indicates that the channels for energy transfer, electron or otherwise, to the molecule are removed when Ag(111) is precovered with iodine. Iodine atoms, at a saturated coverage, occupy all of the threefold sites without a Ag atom beneath;[25] these are believed to be the active surface sites for dissociation of CF_3I. Presumably, the activity of these sites is due to the local electronic structure. Again, the orbital overlap of the iodine with the surface at the threefold sites having an underlying Ag atom does not appear to be sufficient to allow electron transfer to the adsorbate. For example, steric repulsion between I and CF_3I does not allow the latter to react with the metal. More than likely, a combination of both structural changes associated with the overlayer and eliminating certain decomposition sites effectively shuts off the CF_3 radical desorption channels. It is also worth noting that the observed work function for Ag(111) with a saturated coverage of iodine is 0.35 eV higher than for a clean surface,[11] increasing the potential required for DEA.

V. SUMMARY

CF_3I adsorbs molecularly on Ag(111) at 90 K. A minor dissociative adsorption channel limited to C–I bond cleavage is also present. Upon heating an initial coverage of 1 ML, approximately 23% of the CF_3I dissociates and remains adsorbed as CF_3 and I. As reported previously, there is no evidence for C–F bond breakage or C–C bond formation. Some CF_3 thermally desorbs as a radical at high temperatures (~320 K) and saturates at a total coverage of 1 ML. The angular distribution of this desorption channel is fit with a cosine fall-off with increasing angle away from the surface normal. Over a narrow range of coverages ($\leqslant$1 ML CF_3I), a low temperature (100–150 K) CF_3 radical desorption channel appears. This channel saturates at 1 ML CF_3I (0.27 ML CF_3), and its desorption maximum is located ~18° off-normal. Atomic iodine desorbs at approximately 850 K. No CF_3 radical desorption is observed in either temperature regime on I-precovered Ag(111).

Low temperature CF_3 thermal desorption occurs via dissociation of molecular CF_3I, yielding radical CF_3 and adsorbed iodine. Drawing from gas phase scattering and solid state diffraction studies, we propose a model for the mechanism of CF_3 ejection. In the first monolayer, CF_3I molecules adsorb iodine down, forming two-dimensional clusters that loosely resemble the solid state crystalline structure of CF_3I. As the substrate is heated, the molecules reorient, inducing

CF_3 formation via a dissociative electron attachment from the substrate to the adsorbate. Thermally-stimulated DEA occurs through the σ^* molecular orbital in the C–I bond, ejecting CF_3 radicals into the gas phase along the C–I bond axis, leaving I^- on the surface. The tilting of the molecules on the surface lowers the activation barrier for EA and/or opens a tunneling channel through the barrier. This model accounts for both the appearance of low temperature CF_3 radicals and their preferential desorption angle. The CF_3 desorption channels are closed off by precovering the Ag(111) surface with iodine atoms. On the I-passivated surface, the threefold sites believed to be active in the dissociation reaction are occupied by iodine atoms. The change in the local electronic and spatial structure, along with the increase in substrate work function, may all contribute to suppression of CF_3 desorption.

ACKNOWLEDGMENT

This work was supported in part by the National Science Foundation under Grant No. CHE9319640.

[1] P. Zurer, Chemistry and Engineering News (November 14, 1994).
[2] T. Underwood-Lemons, T. J. Gergel, and J. H. Moore, J. Chem. Phys. **102**, 119 (1995).
[3] S. H. Alajajian, K-F. Man, and A. Chutjian, J. Chem. Phys. **94**, 3629 (1991).
[4] (a) M. Heni and E. Illenberger, Chem. Phys. Lett. **131**, 314 (1986); (b) T. Oster, O. Ingolfsson; M. Meinke, T. Jaffke, and E. Illenberger, J. Chem. Phys. **99**, 5141 (1993).
[5] (a) C. W. Walter, B. G. Lindsay, K. A. Smith, and F. B. Dunning, Chem. Phys. Lett. **154**, 409 (1989); (b) R. N. Compton, P. W. Reinhardt, and C. D. Cooper, J. Chem. Phys. **68**, 4360 (1978).
[6] R. G. Jones and N. K. Singh, Vacuum **38**, 213 (1988); J. S. Dyer and P. A. Thiel, Surf. Sci. **238**, 169 (1990).
[7] Z.-M. Liu, X.-L. Zhou, J. Kiss, and J. M. White, Surf. Sci. **286**, 233 (1993).
[8] M. B. Jensen and P. A. Thiel, J. Am. Chem. Soc. **117**, 438 (1995).
[9] (a) M. B. Jensen, U. Myler, C. J. Jenks, P. A. Thiel, E. D. Pylant, and J. M. White, J. Phys. Chem. **99**, 8736 (1995); (b) M. B. Jensen, J. S. Dyer, W.-Y. Leung, and P. A. Thiel (submitted).
[10] K. B. Myli and V. H. Grassian, J. Phys. Chem. **99**, 1498, 5581 (1995).
[11] M. E. Castro, L. A. Pressley, J. Kiss, E. D. Pylant, S. K. Jo, X.-L. Zhou, and J. M. White, J. Phys. Chem. **97**, 8476 (1993), and references therein.
[12] (a) J.-L. Lin and B. E. Bent, J. Am. Chem. Soc. **115**, 2849, (1993); (b) J. Phys. Chem. **97**, 9713 (1993).
[13] (a) V. A. Ukraintsev, T. J. Long, and I. Harrison, J. Chem. Phys. **96**, 3957 (1992); (b) V. A. Ukraintsev, T. J. Long, T. Gowl, and I. Harrison, *ibid*. **96**, 9114 (1992)
[14] (a) S. A. Buntin, L. J. Richter, D. S. King, and R. R. Cavanagh, J. Chem. Phys. **91**, 6429 (1989); (b) X.-Y. Zhu, J. M. White, M. Wolf, E. Hasselbrink, and G. Ertl, J. Phys. Chem. **95**, 8393 (1991); (c) Z. C. Ying and W. Ho, J. Chem. Phys. **94**, 5701 (1991); (d) Q. Y. Yang, W. N. Schwartz, and R. M. Osgood, Jr., *ibid.* **98**, 1008 (1993); (e) St. J. Dixon-Warren, E. T. Jensen, J. C. Polanyi, G.-Q. Xu, S. H. Yang, and H. C. Zeng, Faraday Discuss. Chem. Soc. **91**, 451 (1991); (f) T. L. Gilton, C. P. Dehnbostel, and J. P. Cowin, J. Chem. Phys. **91**, 1937 (1989); (g) Ph. Avouris and R. E. Walkup, Annu. Rev. Phys. Chem. **40**, 173 (1989).
[15] Z.-J. Sun, A. L. Schwaner, and J. M. White, J. Chem. Phys. **103**, 4279 (1995).
[16] (a) P. A. Dowben, CRC Crit. Rev. Solid State Mater. Sci. **13**, 191 (1987); (b) D. R. Herschbach, Adv. Chem. Phys. **10**, 319 (1966).
[17] Z.-J. Sun, S. Gravelle, R. S. Mackay, X.-Y. Zhu, and J. M. White, J. Chem. Phys. **99**, 10 021 (1993).
[18] R. S. Mackay, K. H. Junker, and J. M. White, J. Vac. Sci. Technol. A **12**, 2293 (1994).
[19] *CRC Atlas of Spectral Data and Physical Constants for Organic Compounds*, edited by J. G. Grasselli and W. M. Ritchey (Chemical Rubber, Cleveland, 1975).
[20] L. J. Gerenser and R. C. Baetzold, Surf. Sci. **99**, 259 (1980).
[21] A. Szabo, S. Converse, and J. M. White (submitted).
[22] P. A. Redhead, Vacuum **12**, 203 (1962).
[23] S. J. Clarke, J. K. Cockcroft, and A. N. Fitch, Z. Kristallogr. **206**, 87 (1993).
[24] Jack Tossell (unpublished results).
[25] F. Forstmann, W. Berndt, and P. Buttner, Phys. Rev. Lett. **30**, 17 (1973).
[26] R. J. D. Miller, in *Surface Electron Transfer Processes* (VCH, New York, 1995), Chap. 4.
[27] *CRC Handbook of Chemistry and Physics*, edited by R. C. Weast (Chemical Rubber, Boca Raton, 1989).
[28] L. G. Christophorou, D. L. McCorkle, and A. A. Christodoulides, in *Electron–Molecule Interactions and Their Applications*, edited by L. G. Christophorou (Academic, New York, 1984), Vol. 1.
[29] T. Underwood-Lemons, D. C. Winkler, J. A. Tossell, and J. H. Moore, J. Chem. Phys. **100**, 9117 (1994); estimate supported by private communication with the author.
[30] *Handbook of Organic Solvents*, edited by D. R. Lide (Chemical Rubber, Boca Raton, 1995); The value is approximately equal to an estimated Born value for the polarization energy of a solvated CF_3Cl anion. The dielectric constant for CF_3Cl at $-150\,°C$ is $\epsilon=3.01$, obtained from the aforementioned reference. In this case, $P^-=-1.6$ and for a monolayer coverage $\chi=0.33$.
[31] G. Herzberg, *Electronic Spectra of Polyatomic Molecules* (Van Nostrand Reinhold, New York, 1966); M. B. Robin, *Higher Excited States of Polyatomic Molecules* (Academic, New York, 1974), Vol. 1.